Phase Transformation of Hydrothermally Synthesized Nanoparticle TiO$_2$: from Anatase to Rutile Nanorods

Paul J. Franklyn[a][*], Demetrius C. Levendis[a][*], Neil J. Coville[a] and Malik Maaza[b]

[a] *Molecular Sciences Institute, School of Chemistry, University of the Witwatersrand, Johannesburg, P.O. WITS, 2050 South Africa.*
[b] *School of Physics, University of the Witwatersrand, Johannesburg, P.O. WITS, 2050 South Africa.*

ABSTRACT

Mild hydrothermal hydrolysis of TiCl$_4$ produces nanorods of the rutile phase of titanium dioxide in high yield, while in the presence of organic acids (citric, acetic, D-tartaric and benzoic acids) anatase is the only product. The effect of these organic acids on the products of the hydrolysis reaction as well as the reaction kinetics of the hydrolysis reaction were studied using X-ray powder diffraction and scanning electron microscopy. These studies confirmed that the anatase phase, stabilized by the organic acid, is the kinetically produced product. In addition, in the absence of any organic acids, the conversion of anatase to rutile occurred in two steps (rate constants 0.046 ± 0.025 min^{-1} and 0.0013 ± 0.0002 min^{-1}). The first step entailed a relatively rapid reaction corresponding to the conversion of anatase nanoparticles to rutile nanoparticles, while the second slower reaction converted the remaining anatase material into rutile titania nanorod clusters. A mechanism is proposed for the reaction and compared with other literature proposals.

1. Introduction

There are several bottom-up approaches that have been successfully used for the synthesis of titanium dioxide. These include sol-gel,[1,2] hydrothermal[3–5] (or more generally solva-thermal[6,7]) lyophilization, laser ablation, electrodeposition and a range of templating techniques.[8–10] Detailed studies regarding the effects of temperature, additives, pH and starting material on the synthesis of titanium dioxide have been conducted.[3–5,11–21] Despite this, the reaction mechanism for hydrolysis and the formation of crystalline phases in the hydrothermal synthesis is still not well understood.[22]

Several different mechanisms have been proposed for the reaction. These include dehydration,[5,12] various forms of assisted nucleation,[5,16] surface protection,[15,16,23] and proposals that the reaction can fall under both kinetic and thermodynamic controls.[3,15,22,24] No conclusive study has yet been conducted to select a particular mechanism or set of mechanisms for the reaction.[25] Recent studies have shown that organic acids may be used to control the size of nanoparticles.[26]

In the bulk, rutile is the thermodynamically favoured titania phase.[27] However, thermodynamic calculations by Zhang and Banfield have shown that effects associated with the large surface area of nanoparticles can cause a reversal in the relative stability of the anatase and rutile phases compared with the bulk material.[28] From the calculations, Zhang and Banfield determined that for titania particles with diameter <14 nm, anatase is expected to be the more stable phase up to relatively high temperatures. In more recent work the effect of the surface and the size of the particles has been studied further through simulation.[28]

Kinetic studies on the solid phase transformation of anatase and rutile titania in both crystalline[29–31] and amorphous[32,33] forms have been extensively reported. While many studies have reported reaction rates for the phase changes that occur in a gaseous environment (from solid precursors prepared primarily *via* the sol-gel route), very few kinetic studies on the formation and interconversion of anatase or rutile titania in a *hydrothermal synthesis* have been reported.[34,35] The determination of these reaction rates is important since the kinetic expressions obtained will permit control of the synthesis of the prepared nanoparticles, and hence contribute to establishing procedures to favour the respective titania phases. Kinetic studies on nanoparticles have also shown that the size can affect the rates of the transformation.[36] Further, an understanding of the mechanism of the reaction will allow for control of the anatase and rutile ratios that in turn will allow for control of the properties of the resulting materials.

In the work presented here, the kinetics and mechanism of the formation of anatase nanoparticles in a hydrothermal synthesis starting from a TiCl$_4$ precursor and the subsequent conversion of the particles to rutile nanorods were studied.

2. Experimental

2.1. Effect of Organic Acids

Titanium tetrachloride (99%, Aldrich) was added dropwise (~1.5 mL min^{-1}) from a 10 mL glass syringe to a flask containing 30 mL iced distilled water with vigorous stirring using a magnetic stirrer bar. Various organic acids (citric, acetic, D-tartaric and benzoic acids; see Table 1 for concentrations) were also added to this mixture. The mixture was then refluxed for 20 h in an oil bath set at 220 °C. Powder samples were collected by centrifugation of the reaction mixture. The supernatant was poured off and the precipitate re-suspended in distilled water and then centrifuged again and the process repeated several times to wash the powders. Finally the powders were evaporated to dryness in an oven at 45 °C.

* To whom correspondence should be addressed. E-mail: pjfranklyn@gmail.com (Franklyn), demi@chem.wits.ac.za (Levendis).

Table 1 Organic acids used.[a]

Acid	Amount/mol	Concentration / mol L^{-1}	Phase produced
None	–	–	Rutile
Acetic acid	0.2446	8.153	Anatase
Benzoic acid	0.06171	2.057	Anatase
Citric acid	0.02057	0.6857	Anatase
D-Tartaric acid	0.02094	0.6980	Anatase

[a]Amount Ti used = 0.0273 mol.

Table 2 Amount of citric acid added and phase ratio.

Amount of acid/mol	Ratio of TiCl$_4$ to organic acid	Mass % anatase: rutile	Average particle size of anatase/nm
2.057×10^{-2}	1.327	100:0	6
7.756×10^{-3}	3.519	100:0	6
2.551×10^{-3}	10.7	99:1	5
6.402×10^{-4}	42.64	93:7	6
3.227×10^{-4}	84.59	74:26	5

Table 3 Amount of acetic acid added and phase ratio.

Amount of acid/mol	Ratio of TiCl$_4$ to organic acid	Mass % anatase: rutile	Average particle size of anatase /nm
0.2446 (no water)	0.1116	100:0[a]	5
0.2446	0.1116	100:0	6
0.1223	0.2232	39:61	6
0.06114	0.4465	34:66	5
0.02096	1.302	0:100	–

[a]A small amount of brookite was also present in this sample.

2.2. Kinetic Experiments

Kinetic experiments were performed by adding 0.33 mol TiCl$_4$ (at about 1.5 mL min^{-1}) to 360 mL of iced distilled water with vigorous stirring. No organic acid was added. The mixture was then refluxed and, after 45 min, 15 mL aliquots were withdrawn from the reaction mixture every 30 min for the next 525 min. Further 15 mL aliquots of the reaction solution were collected after 675, 1365, 1665 and 2880 min. Each aliquot was centrifuged and washed once before being evaporated to dryness. The samples were then analysed.

2.3. Analysis

The powder samples were characterized by powder X-ray diffraction (PXRD) using a Philips PW1820 powder X-ray diffractometer (to determine the anatase:rutile phase ratio) by stepping at 0.01 ° 2θ and counting for 6 s per step. The sample area irradiated was 144 mm^2, controlled using a variable slit width linked to the 2θ motor. The mass percentage anatase in each sample was determined from PXRD patterns using the relationship:[37]

$$x_A = [1 + 1.26(I_R/I_A)]^{-1}$$

(error bar 5% by mass), where I_R and I_A refer to the maximum intensities of the rutile (110) and anatase (101) peaks, respectively. Particle sizes were calculated using the Debye-Scherrer equation[38,39] with a k value of 0.91. The calculation included a machine-broadening component in the FWHM found using a large-grain silicon standard supplied with the diffractometer. High-resolution scanning electron microscopy (SEM) was used to evaluate the particle morphology and was carried out on a JEOL JSM-6000F SEM.

3. Results and Discussion

3.1. Effect of Organic Acids

It has been suggested that organic acids play a role in controlling the product of the TiCl$_4$ hydrolysis reaction.[5,15,16,23] To test this acid effect, a short-chain acid (acetic acid), a bulkier and hydrophobic acid (benzoic acid), and acids with carboxyl and hydroxyl groups (citric and D-tartaric acids) were used. A standard reaction was also performed without organic acid addition. The samples were prepared using 0.0273 mol of TiCl$_4$ in 30.0 mL distilled water and the amount of each organic acid was varied to keep the ratio of oxygen donor atoms to Ti atoms approximately constant, except for acetic acid where an excess was used (see Table 1).

As seen in Table 1, the presence of *all* the organic acids in sufficiently high concentration resulted in the formation of anatase exclusively, with the same macroscopic morphology observed for all samples. The phase of the titania was determined by PXRD. In the absence of organic acid, only rutile was formed. The rutile that was produced was formed as nanorods (up to

100 nm long and 5–10 nm thick as observed in HRSEM) arranged in radially aligned clusters to create large balls of titania.

The relative amounts of organic acid (citric and acetic acids) influenced the titania anatase:rutile phase ratio as detected by XRD (see Tables 2 and 3). It is apparent from the results that the Ti:organic acid ratio plays a role in influencing the amount but not the particle size of the anatase produced. The particle size was always approximately 6 nm in diameter, independent of the Ti:organic acid ratio and independent of the organic acid used. As the amount of organic acid was decreased, the amount of rutile produced increased. No effect on the particle morphology of the anatase was observed as the concentration of organic acid was decreased. Further, the rutile formed was rod-like, regardless of the concentration of citric acid used. It was also found that reduction of both the concentration of TiCl$_4$ and citric acid (but with the ratio TiCl$_4$:organic acid unchanged) did not affect the synthesis and that with sufficient organic acid present, anatase was formed exclusively.[25]

This confirms that the organic acid plays a crucial role in the synthetic process. Based on the results of Bangfield and Zhang[27] anatase nanoparticles of small size should have been thermodynamically stable. However, in the hydrothermal environment this stability is altered and rutile is the preferred product. In the acidic hydrothermal environment the binding of hydroxyl and proton species to the surface of the particles may serve to stabilize the surface of anatase and hence reduce the surface Gibbs energy that is attributed to making anatase the more stable phase.

This finding can also explain the contradictory reports found in the literature on the formation of anatase versus rutile phases of titania under apparently identical reaction conditions in the presence of acids. The results can be explained by considering surface capping of the anatase nanoparticles by the organic acid. If insufficient organic acid is used (or if the organic acid is poorly soluble) incomplete protection of the synthesized anatase will occur and rutile formation will dominate. In the presence of large amounts of organic acids (when surface capping is complete) the phase conversion reaction rates will be slow. In excess organic acid the surface capping action will be complete.
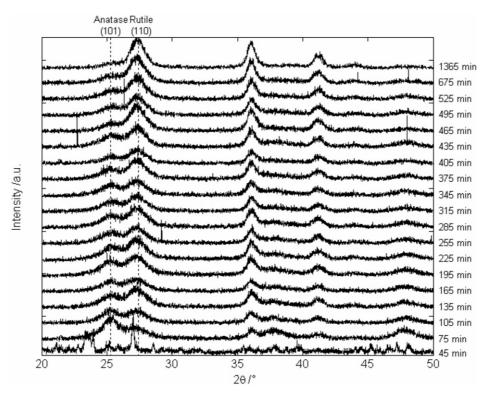
Figure 1 PXRD patterns of the samples showing the formation of anatase from a complex precursor and the conversion of anatase to rutile. This conversion is observed through the changing ratios of the maximum intensity of the anatase (101) Bragg peak at 25.4 ° 2θ and the rutile (110) peak at 27.5 ° 2θ.

3.2. Kinetic Experiments

The hydrolysis of $TiCl_4$ in the absence of any organic acids was monitored by PXRD (see Fig. 1). It can be seen in Fig. 1 that the first sample collected (45 min) revealed the presence of neither anatase nor rutile phases (peaks were observed in the PXRD neither at the (101) position of anatase nor at the (110) position of rutile as marked on the figure). The identity of the material is unknown, but it is assumed to be either a titanate or a mixture of titanium oxychloride species (see below). The conversion reaction of the unidentified component to anatase was not monitored but found to be extremely rapid relative to the subsequent anatase/rutile transformation reaction, going from start to completion in less than 30 min (comparison of PXRD patterns at 45 min and 75 min; Fig. 1). In the pattern collected at 45 min only the unidentifiable component is present. In the XRD patterns of the samples collected after 75 min, none of this component was observed.

Figure 2 shows the conversion of anatase to rutile by plotting the mass percentage of anatase as a function of time. A two-term exponential fit ($y = ae^{-bx} + ce^{-dx}$ with parameters $a = 792 \pm 1478$, $b = 0.046 \pm 0.025$, $c = 60 \pm 3$, $d = 0.0013 \pm 0.0002$) was obtained for the data with a goodness of fit of 97%. It is proposed that the two reaction rates can be attributed to the initial conversion of the nanoparticles of anatase to rutile ($k = 0.046 \pm 0.025$ min^{-1}, a
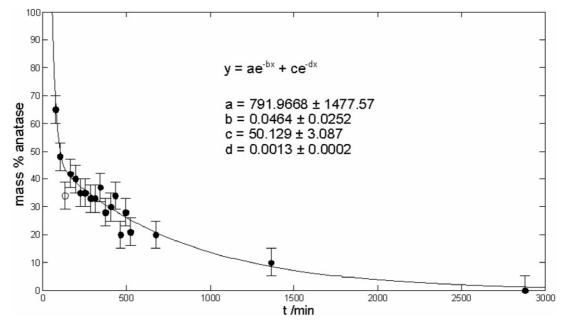

$$y = ae^{-bx} + ce^{-dx}$$

$a = 791.9668 \pm 1477.57$
$b = 0.0464 \pm 0.0252$
$c = 50.129 \pm 3.087$
$d = 0.0013 \pm 0.0002$

Figure 2 A two-term exponential fit of the mass percentage anatase, determined from PXRD analysis, plotted against the reaction time.
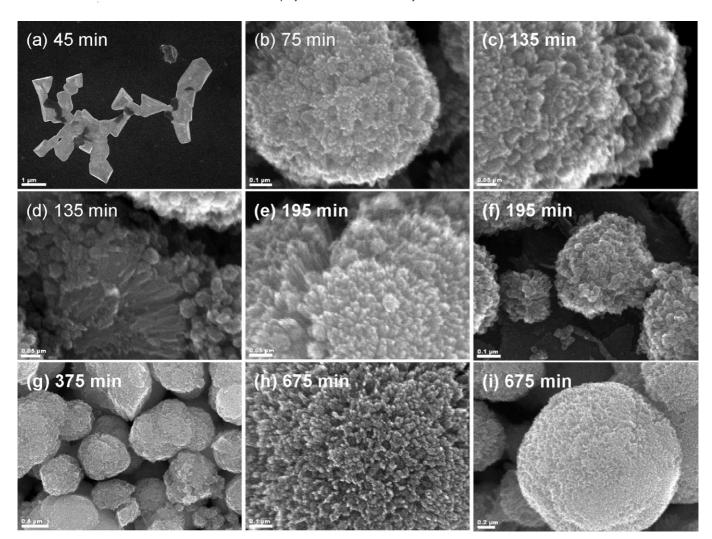
Figure 3 SEM images of samples after selected reaction times (scale bar for each image given in brackets: (**a**) 45 min (1 μm), surface featureless and material not TiO$_2$; (**b**) 75 min (0.1 μm), balls of primarily anatase nanoparticles; (**c**) 135 min (0.05 μm), balls of nanoparticles; (**d**) 135 min (0.05 μm); (**e**) 195 min (0.05 μm); (**f**) 195 min (0.1 μm); (**g**) 375 min (0.5 μm); (**h**) 675 min (0.1 μm), clusters of rods of rutile; (**i**) 675 min (0.2 μm), clusters of rods of rutile.

relatively rapid process) followed by the growth process of the rods (k = 0.0013 ± 0.0002 min^{-1}, a much slower process).

SEM images of the products were also collected as a function of time (see Fig. 3). The SEM image of the sample collected after 45 min of reaction is shown in Fig. 3a. This sample exhibited electron beam damage that is not observed with titanium dioxide. Combined with the PXRD results it can be confirmed that the material that had formed is thus not titanium dioxide (anatase or rutile). SEM measurements performed on all the other samples from the rest of the experiment did not sustain electron beam damage.

SEM analysis of the sample synthesized after 75 min of reaction revealed clusters of well-defined nanoparticles. The SEM analysis of the samples collected at 75 and 105 min after the start of the reaction revealed that less than 30% of the sample comprised rod-like material. It was expected that these rods are composed entirely of rutile, based on the results reported above with the organic acids (see also Yin *et al.*[16]).

Further analysis of the SEM images showed that after the initial changes (45–75 min), the product showed a progressive change in the morphology and shape, but not of the clustering of the nanoparticles in the samples (see Fig. 3b–i). Over the duration of the experiment SEM analysis of all the samples showed that the clusters of nanoparticles initially observed in the 75 min sample appeared to convert directly into clusters of radially aligned nanorods. It can be seen that the sample converts directly from the clusters of nanoparticles of anatase (~5 nm diameter) into clusters of radially aligned nanorods of rutile (~8 nm diameter and ~100 nm in length).[16,25]

Analysis of the samples by (i) PXRD patterns between 105 min and 195 min (where it was observed that the mass percentage of rutile in the sample was in excess of 50%) and (ii) SEM (where more that 50% of the observed material was not rod-like) reveals that some of the anatase nanoparticles first undergo a phase change to rutile *and are then* converted into rods. Note that during this time period the crystallite sizes of the anatase and rutile are proportional and around 6 nm for anatase and 12 nm for rutile (in the direction of growth of the rods).

This kinetic study reveals that the organic acid is not essential for the formation of anatase and that anatase is the kinetic product of the hydrolysis reaction. Therefore, assisted nucleation mechanisms for the role of the organic acid can be ruled out, leaving acid promoted dehydration of hydroxyl-complexed titanium ions as the primary route for anatase formation.[25] In addition this result indicates a thermodynamic drive for the formation of rutile.

Thus, given the data that we have presented here, we propose that the formation of anatase occurs through a hydrothermal

dehydration reaction of the titanium ions complexed with water, hydroxyl species and chloride ions, resulting from the dissolution of $TiCl_4$ in water. Further it is proposed that the initial rapid conversion of anatase nanoparticles to rutile nanoparticles occurs according to the interface mechanisms between adjacent nanoparticles of anatase as suggested by others.[30–33] This is known to be a relatively rapid process and correlates well with the initial faster rate of the reaction observed in this study.

It is finally postulated that the slow growth process is achieved in one of two ways. The first is through dissolution of the anatase crystals followed by recrystallization in the rutile phase at the ends of the rods. The second is through the unconverted anatase nanoparticles interacting directly with the surface of the existing rutile nanorods and hence reacting to form rutile.[29] Further experimental work (*in situ* PXRD and more detailed TEM and SEM analysis) would be required to differentiate between these postulates.

4. Conclusion

The experimental work conducted here indicates that multiple processes take place in the hydrothermal hydrolysis of $TiCl_4$. The first is the rapid formation of unknown Ti-containing species. The second reaction involves the formation of anatase from these precursors. This is followed by the conversion of anatase to rutile that could be hindered or even stopped by the addition of an organic acid. The final reaction involved the slow conversion of anatase to rutile, accompanied by the growth of nanorods of rutile.

The growth of nanorods of rutile was not hindered by the presence of organic acids. The rate constant for the conversion of anatase nanoparticles to rutile nanorods was found to be $0.046 \pm 0.025 \ min^{-1}$ and the rate constant for the growth of the rutile rods was found to be $0.0013 \pm 0.0002 \ min^{-1}$. Finally the presence of an organic acid limits the interaction of water with the surface-capped anatase nanoparticles and also limits interaction between neighbouring nanoparticles. Such interaction would prevent the reaction of anatase from forming rutile.

References

1 T. Sugimoto, X. Zhou and A. Muramatsu, *J. Colloid Interface Sci.,* 2003, **259,** 43–52.

2 T. Sugimoto, X. Zhou and A. Muramatsu, *J. Colloid Interface Sci.,* 2003, **259,** 53–61.

3 Y. Li, Y. Fan and Y. Chen, *J. Mater. Chem.,* 2002, **12,** 1387–1390.

4 H. Kominami, M. Kohno, Y. Takada, M. Inoue, T. Inui and Y. Kera, *Ind. Eng. Chem. Res.,* 1999, **38,** 3925–3931.

5 H. Yin, Y. Wada, T. Kitamura, S. Kambe, S. Murasawa, H. Mori, T. Sakata and S. Yanagida, *J. Mater. Chem.,* 2001, **11,** 1694–1703.

6 C. Wang, Z-X. Deng and Y. Li, *Inorg. Chem.,* 2001, **40,** 5210–5214.

7 C-S. Kim, B.K. Moon, J-H. Park, S.T. Chung and S-M. Son, *J. Cryst. Growth,* 2003, **254** , 405–410.

8 T-Z. Ren, Z-Y. Yuan and B-L. Su, *Chem. Phys. Lett.,* 2003, **374,** 170–175.

9 D.K. Yi and D-Y. Kim, *Nano Lett.,* 2003, **3,** 207–211.

10 T. Peng, A. Hasegawa, J. Qiu and K. Hirao, *Chem. Mater.,* 2003, **15,** 2011–2016.

11 T. Moritz, J. Reiss, K. Diesner, D. Su and A. Chemseddine, *J. Phys. Chem. B,* 1997, **101,** 8052–8053.

12 K. Yanagisawa and J. Ovenstone, *J. Phys. Chem. B,* 1999, **103,** 7781–7787.

13 R.L. Penn and J.F. Banfield, *Am. Mineral.,* 1998, **83,** 1077–1082.

14 C-C. Wang and J.Y. Ying, *Chem. Mater.,* 1999, **11,** 3113–3120.

15 M. Wu, G. Lin, D. Chen, G. Wang, D. He, S. Feng and R. Xu, *Chem. Mater.,* 2002, **14,** 1974–1980.

16 H. Yin, Y. Wada, T. Kitamura, T. Sumida, Y. Hasegawa and S. Yanagida, *J. Mater. Chem.,* 2002, **2,** 378–383.

17 Q. Zhang and L. Gao, *Langmuir,* 2003, **19,** 967–971.

18 C-S. Fang and Y-W. Chen, *Mater. Chem. Phys.,* 2003, **78,** 739–745.

19 J. Lin, Y. Lin, P. Liu, M.J. Meziani, L.F. Allard and Y-P. Sun, *J. Am. Chem. Soc.,* 2002, **124,** 11514–11518.

20 Y. Wej, R. Wu and Y. Zhang, *Mater. Lett.,* 1999, **41,** 101–103.

21 B. Xia, H. Huang and Y. Xie, *Mater. Sci. Eng. B,* 1999, **57,** 150–154.

22 H.B. Weiser, W.O. Milligan and E.L. Cook, *J. Phys. Chem.* 1941, **45** 1227–1234.

23 J-P. Hsu, and A. Nacu, *Langmuir,* 2003, **19,** 4448–4454.

24 K. Yang, J. Zhu, J. Zhu, S. Huang, X. Zhu and G. Ma, *Mater. Lett.,* 2003, **57,** 4639–4642.

25 P.J. Franklyn, *Hydrothermal Synthesis and Characterisation of Titania Nanoparticles,* M.Sc. thesis, University of the Witwatersrand, Johannesburg, 2004.

26 B. Jiang, H. Yin, T. Jiang, J. Yan, Z. Fan, C. Li, J. Wu and Y. Wada, *Mater. Chem. Phys.,* 2005, **92,** 595–599.

27 H. Zhang and J.F. Banfield, *J. Mater. Chem.,* 1998, **8,** 2073–2076.

28 P.K. Naicker, P.T. Cummings, H. Zhang and J.F. Banfield, *J. Phys. Chem. B,* 2005, **109,** 15243–15249.

29 A.A. Gribb and J.F. Banfield, *Am. Mineral.,* 1997, **82,** 717–728.

30 H. Zhang and J.F. Banfield, *Am. Mineral.,* 1999, **84,** 528–535.

31 Y. Hu, H-L. Tsai and C-L. Huang, *J. Eur. Ceram. Soc.,* 2003, **23,** 691–696.

32 P.S. Ha, H-J. Youn, H.S. Jung, K.S. Hong, Y.H. Park and K.H. Ko, *J. Colloid Interface Sci.,* 2000, **223,** 16–20.

33 H. Zhang and J.F. Banfield, *Chem. Mater.,* 2002, **14,** 4145–4154.

34 S. Sathyamoorthy, G.D. Moggridge and M.J. Hounslow, *Cryst. Growth Des.,* 2001, **1,** 123–129.

35 H. Cheng, J. Ma, Z. Zhao and L. Qi, *Chem. Mater.,* 1995, **7,** 663–671.

36 H. Zhang and J.F. Banfield, *Chem. Mater.,* 2005, **17,** 3421–3425.

37 R.A. Spurr and H. Myers, *Anal. Chem.,* 1957, **29,** 760–762.

38 B.E. Warren, *X-ray Diffraction,* Addison Wesley Publishing Company, Reading, MA, 1969.

39 H.P. Klug and L.E. Alexander, *X-ray Diffraction Procedures for Polycrystalline and Amorphous Materials,* 2nd edn. John Wiley & Sons, New York, 1974.